ELSEVIER

Journal of Fluids and Structures 26 (2010) 804–813

JOURNAL OF FLUIDS AND STRUCTURES

www.elsevier.com/locate/jfs

Brief Communication

Dynamics of pipes conveying fluid with non-uniform turbulent and laminar velocity profiles

A.M. Hellum[a], R. Mukherjee[a,*], A.J. Hull[b]

[a]*Department of Mechanical Engineering, 2555 Engineering Building, Michigan State University, East Lansing, MI 48824-1226, USA*
[b]*Advanced Acoustic Systems Division, Autonomous and Defensive Systems Department, Naval Undersea Warfare Center, Newport, RI 02841, USA*

Received 29 December 2009; accepted 4 May 2010
Available online 19 June 2010

Abstract

Previous analytical work on stability of fluid-conveying pipes assumed a uniform velocity profile for the conveyed fluid. In real fluid flows, the presence of viscosity leads to a sheared region near the wall. Earlier studies correctly note that viscous forces do not affect the dynamics of the system since these forces are balanced by pressure drop in the conveyed fluid. Although viscous shear has not been ignored in these studies, a uniform velocity profile assumes that the sheared region is infinitely thin. Prior analysis was extended to account for a fully developed non-uniform profile such as would be encountered in real fluid flows. A modified, highly tractable equation of motion was derived, which includes a single additional parameter to account for the true momentum of the fluid. This empirical parameter was determined by numerical analysis over the Reynolds number range of interest. The stability of cantilever pipes conveying fluid with two types of non-uniform velocity profile was assessed. In the first case, the profile was a function of Reynolds number and transition to turbulence occurred before the onset of flutter instability. This case had stability properties similar to the uniform velocity case except in specific narrow regions of the parameter space. The second case required that the Reynolds number be such that the flow was always laminar. For this case, lower fluid velocity was required to achieve instability, and the oscillation frequency at instability was considerably lower over much of the parameter space, compared to the uniform case.

Keywords: Fluid-conveying pipe; Non-uniform velocity profile; Internal flow; Flutter; Instability; Laminar flow; Viscous flow

1. Introduction

The study of the dynamics of fluid-conveying pipes can be traced to Bourrières (1939), who carried out theoretical and experimental investigations of instability of a cantilevered pipe conveying fluid. The problem was revisited by Ashley and Haviland (1950) a decade later, following observations of vibration in the Trans-Arabian pipeline. A large volume of research has been done since then by Païdoussis and co-workers, and his review paper (Païdoussis and Li, 1993) provides an excellent introduction to the topic. A review of the literature of fluid-conveying pipes indicates that all

*Corresponding author. Tel.: +1 517 355 1834; fax: +1 517 353 1750.
E-mail addresses: hellumar@egr.msu.edu (A.M. Hellum), mukherji@egr.msu.edu (R. Mukherjee), andrew.hull@navy.mil (A.J. Hull).

0889-9746/$ - see front matter © 2010 Elsevier Ltd. All rights reserved.
doi:10.1016/j.jfluidstructs.2010.05.001

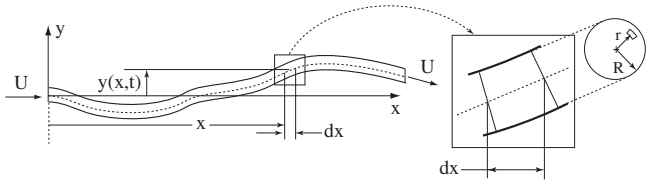

Fig. 1. A fluid-conveying pipe and a magnified view of a small length element.

standard formulations of the problem have been investigated. The pinned–pinned boundary condition was studied by Feodoseev (1951) and Housner (1952) and the cantilever problem was investigated by Bourrières (1939) and Gregory and Païdoussis (1966). Other researchers extended the analysis to include Timoshenko beam models (Païdoussis and Laithier, 1976), nonlinear formulations (Bajaj et al., 1980; Holmes, 1978; Lundgren et al., 1979), external flows (Hannoyer and Païdoussis, 1978), unsteady flows (Païdoussis and Issid, 1974), and many other effects.

The assumption of plug flow is ubiquitous in analytical treatments of the problem. Under this assumption, the velocity profile is uniform across the cross-section of the pipe. This assumption may be justified for a given system with the observation that at high Reynolds number, the velocity profile is nearly uniform over the central region of the cross-section, with only a thin, highly sheared annular region near the pipe wall. The plug flow assumption is less valid at low Reynolds numbers, particularly if the flow is laminar. For a given working fluid and a pipe with given dimensions and material properties, the Reynolds number uniquely defines a value for the relevant nondimensional velocity, but this is not true in the general case. In this paper we have generalized the results of previous work to account for non-uniform flow, both in the cases of non-ideal turbulent flow and laminar flow.

This paper is organized as follows. The equation of motion of a pipe conveying fluid with a uniform velocity profile (plug flow) is presented in Section 2 as background material. The derivation of plug flow is extended to a non-uniform velocity profile in Section 3. A triple plug flow model is first studied and then extended to N-plug flow which can be used to model an arbitrary velocity profile for large values of N. The resulting equation for the non-uniform flow differs from the standard equation for uniform flow by a single constant; it is highly tractable, requiring no more effort to solve than the standard equation. This constant, a momentum correction factor,[1] is determined in Section 4. The uniform and non-uniform flow equations for a cantilever pipe are solved in Section 4 and the results are compared in Section 5 for both laminar and turbulent flow. Concluding remarks are provided in Section 6.

2. Background—Uniform velocity profile

Consider the fluid-conveying pipe in Fig. 1 where U denotes the fluid velocity (constant) relative to the pipe. Assuming an Euler–Bernoulli beam model of the pipe, its equation of motion [see Païdoussis (1998) for details] can be written as follows:

$$EI\frac{\partial^4 y}{\partial x^4}+MU^2\frac{\partial^2 y}{\partial x^2}+2MU\frac{\partial^2 y}{\partial x\partial t}+(M+m)\frac{\partial^2 y}{\partial t^2}=0, \tag{1}$$

where E and I are Young's modulus of elasticity and area moment of inertia of the cross-section of the pipe; and M and m are the fluid mass and pipe mass per unit length. The above equation can be obtained by showing that the rate of change of linear momentum of a fluid element is given by the expression (Païdoussis, 1998)

$$\frac{\mathrm{d}\vec{L}}{\mathrm{d}t}=M\left[\frac{\partial}{\partial t}+U\frac{\partial}{\partial x}\right]^2 y\,\mathrm{d}x\hat{j}, \tag{2}$$

and from the equations of motion of a fluid element and its corresponding pipe element (see Fig. 2) in the x and y directions

$$-A\frac{\partial p}{\partial x}-qS-F\frac{\partial y}{\partial x}=0, \tag{3}$$

$$F-A\frac{\partial}{\partial x}\left(p\frac{\partial y}{\partial x}\right)-qS\frac{\partial y}{\partial x}=M\left[\frac{\partial}{\partial t}+U\frac{\partial}{\partial x}\right]^2 y, \tag{4}$$

[1]The momentum correction factor has appeared in the fluid mechanics literature earlier (Benedict, 1980).

$$\frac{\partial T}{\partial x} + qS + F\frac{\partial y}{\partial x} - Q\frac{\partial^2 y}{\partial x^2} = 0, \tag{5}$$

$$\frac{\partial Q}{\partial x} - F + \frac{\partial}{\partial x}\left(T\frac{\partial y}{\partial x}\right) + qS\frac{\partial y}{\partial x} = m\frac{\partial^2 y}{\partial t^2}. \tag{6}$$

In Eqs. (3)–(6), A denotes the cross-sectional area of the pipe, S denotes its internal surface area per unit length, p denotes the fluid pressure, q denotes the shear stress in the fluid, and F denotes the force per unit length normal to the wall. For the pipe element, Q, $\mathbb{M}$ and T denote the traverse shear force, bending moment, and tension, respectively.

3. Non-uniform velocity profile

3.1. Triple plug flow model

The triple plug flow model assumes three concentric volumes of fluid being conveyed through the pipe; the cross-sectional area of these volumes are shown in Fig. 3. The flow velocity is different for the three volumes but is assumed to be constant within each volume. The triple plug flow is not physically realizable, but its analysis provides the framework for investigation of a general velocity profile. Note that the fluid volume at the center (marked 1 in Fig. 3) has a single fluid–fluid interface; the volume in the middle (marked 2 in Fig. 3) has two fluid–fluid interfaces; and the outermost fluid volume (marked 3 in Fig. 3) has one fluid–fluid and one fluid–pipe interface. The analysis for a general velocity profile will require us to introduce more volumes with two fluid–fluid interfaces, similar to volume 2. It is for this reason that three "plugs" are required; using fewer does not give rise to volumes with two fluid–fluid interfaces, and using more creates redundant elements.

To extend the analysis of plug flow in Section 2 to triple plug flow, we denote the cross-sectional areas of volumes 1, 2, and 3 as A_1, A_2 and A_3, respectively; their flow velocities as U_1, U_2 and U_3, respectively; and their mass per unit length as M_1, M_2 and M_3, respectively. F_{12}, F_{23} and F_{3p} denote the radial force per unit length between fluid volumes 1 and 2, fluid volumes 2 and 3, and fluid volume 3 and the pipe, respectively. The shear force at these interfaces are denoted by q_{12}, q_{23} and q_{3p}, respectively, and the surface area per unit length of these interfaces are denoted by S_{12}, S_{23} and S_{3p}, respectively. The dynamics of the fluid volumes 1–3 can now be replicated from Eqs. (3) and (4), and that of the pipe from Eqs. (5) and (6), as follows:

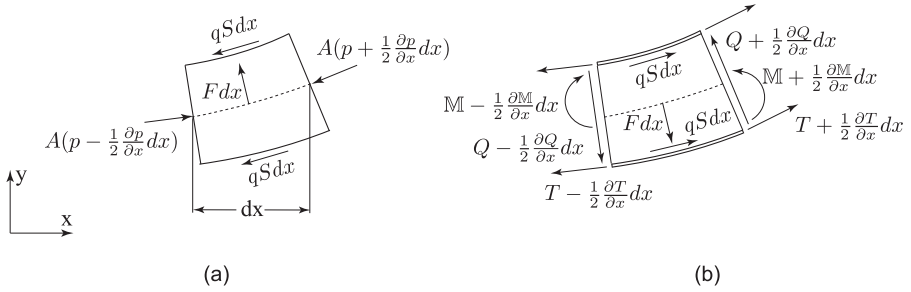

Fig. 2. Free-body diagram of (a) a fluid element and (b) its corresponding pipe element.

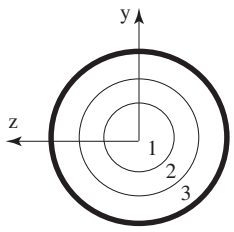

Fig. 3. A cross-sectional view of the three fluid volumes of a triple plug flow.

Volume 1:

$$-A_1\frac{\partial p}{\partial x}-q_{12}S_{12}-F_{12}\frac{\partial y}{\partial x}=0, \tag{7}$$

$$F_{12}-pA_1\frac{\partial^2 y}{\partial x^2}-q_{12}S_{12}\frac{\partial y}{\partial x}=M_1\left[\frac{\partial}{\partial t}+U_2\frac{\partial}{\partial x}\right]^2 y; \tag{8}$$

Volume 2:

$$-A_2\frac{\partial p}{\partial x}-q_{23}S_{23}+q_{12}S_{12}-(F_{23}-F_{12})\frac{\partial y}{\partial x}=0, \tag{9}$$

$$(F_{23}-F_{12})-pA_2\frac{\partial^2 y}{\partial x^2}-(q_{23}S_{23}-q_{12}S_{12})\frac{\partial y}{\partial x}=M_2\left[\frac{\partial}{\partial t}+U_2\frac{\partial}{\partial x}\right]^2 y; \tag{10}$$

Volume 3:

$$-A_3\frac{\partial p}{\partial x}-q_{3p}S_{3p}+q_{23}S_{23}-(F_{3p}-F_{23})\frac{\partial y}{\partial x}=0, \tag{11}$$

$$(F_{3p}-F_{23})-pA_3\frac{\partial^2 y}{\partial x^2}-(q_{3p}S_{3p}-q_{23}S_{23})\frac{\partial y}{\partial x}=M_3\left[\frac{\partial}{\partial t}+U_3\frac{\partial}{\partial x}\right]^2 y; \tag{12}$$

Pipe:

$$\frac{\partial T}{\partial x}+q_{3p}S_{3p}+F_{3p}\frac{\partial y}{\partial x}-Q\frac{\partial^2 y}{\partial x^2}=0, \tag{13}$$

$$\frac{\partial Q}{\partial x}-F_{3p}+T\frac{\partial^2 y}{\partial x^2}+q_{3p}S_{3p}\frac{\partial y}{\partial x}=m\frac{\partial^2 y}{\partial t^2}. \tag{14}$$

The summation of equations in the x direction, namely Eqs. (7), (9), (11) and (13), gives

$$-(A_1+A_2+A_3)\frac{\partial p}{\partial x}+\frac{\partial T}{\partial x}=0. \tag{15}$$

Note that $(A_1 + A_2 + A_3) = A$, where A is the inner cross-sectional area of the pipe. For $A \neq A(x)$, we have from Eq. (15)

$$\frac{\partial}{\partial x}(T-pA)=0, \tag{16}$$

which is the same as that of plug flow (Païdoussis, 1998). The summation of equations in the y direction, namely (8), (10), (12) and (14), gives

$$-pA\frac{\partial^2 y}{\partial x^2}+\frac{\partial Q}{\partial x}+T\frac{\partial^2 y}{\partial x^2}=\sum_{n=1}^{3}M_n\left[\frac{\partial}{\partial t}+U_n\frac{\partial}{\partial x}\right]^2 y+m\frac{\partial^2 y}{\partial t^2}. \tag{17}$$

Following the derivation of plug flow (Païdoussis, 1998) and substituting $(T-pA)=0$ and $Q=-EI(\partial^3 y/\partial x^3)$ into Eq. (17) we get

$$EI\frac{\partial^4 y}{\partial x^4}+\left(\sum_{n=1}^{3}M_nU_n^2\right)\frac{\partial^2 y}{\partial x^2}+2\left(\sum_{n=1}^{3}M_nU_n\right)\frac{\partial^2 y}{\partial x\partial t}+\left(m+\sum_{n=1}^{3}M_n\right)\frac{\partial^2 y}{\partial t^2}=0. \tag{18}$$

3.2. N-plug flow model

It is simple to envision the analysis of the preceding section with more volumes. The additional volumes, similar to volume 2 of triple plug flow in that they possess two fluid–fluid interfaces, do not complicate the analysis since all

interfacial terms are cancelled. Thus Eq. (18) can be rewritten as

$$EI\frac{\partial^4 y}{\partial x^4}+\left(\sum_{n=1}^{N} M_n U_n^2\right)\frac{\partial^2 y}{\partial x^2}+2\left(\sum_{n=1}^{N} M_n U_n\right)\frac{\partial^2 y}{\partial x\partial t}+\left(m+\sum_{n=1}^{N} M_n\right)\frac{\partial^2 y}{\partial t^2}=0, \tag{19}$$

where N is any integer greater than three. For very large values of N, the volumes have infinitesimal thickness and the summations in the coefficients of Eq. (19) can be replaced with integrals. If we define the average velocity of fluid as

$$\overline{U}=\frac{1}{A}\iint_A U(A)\,\mathrm{d}A, \tag{20}$$

for a cylindrical pipe of radius R, we have

$$\overline{U}=\frac{2}{R^2}\int_0^R U(r)r\,\mathrm{d}r. \tag{21}$$

The coefficients of the dynamical equation in Eq. (19) can now be expressed as

$$\left(\sum_{n=1}^{N} M_n U_n^2\right)=\rho_f\iint_A U^2(A)\,\mathrm{d}A=2\pi\rho_f\int_0^R U^2(r)r\,\mathrm{d}r=\mu M\overline{U}^2,$$

$$2\left(\sum_{n=1}^{N} M_n U_n\right)=2\rho_f\iint_A U(A)\,\mathrm{d}A=2\rho_f A\overline{U}=2M\overline{U},$$

$$\left(m+\sum_{n=1}^{N} M_n\right)=m+M, \tag{22}$$

where ρ_f is the density of the conveyed fluid, and μ is the nondimensional momentum correction factor. For a cylindrical pipe with a known fluid velocity profile $U(r)$, μ has the expression

$$\mu=\frac{2}{R^2}\int_0^R\left[\frac{U(r)}{\overline{U}}\right]^2 r\,\mathrm{d}r. \tag{23}$$

It is worth noting that for a uniform velocity profile, $\mu=1$. Using the algebraic simplifications in Eq. (22), Eq. (19) can be rewritten as follows:

$$EI\frac{\partial^4 y}{\partial x^4}+\mu M\overline{U}^2\frac{\partial^2 y}{\partial x^2}+2M\overline{U}\frac{\partial^2 y}{\partial x\partial t}+(m+M)\frac{\partial^2 y}{\partial t^2}=0. \tag{24}$$

Note the similarity of Eq. (24) with that of plug flow given by Eq. (1). All terms are essentially identical with the exception of the additional constant μ, which is a function of the velocity profile.

4. Analysis of a cantilever pipe

4.1. Solution of the differential equation

We analyze the behavior of a fluid-conveying pipe for cantilever boundary conditions, namely

$$y(0,t)=0,\quad y_x(0,t)=0,\quad y_{xx}(L,t)=0,\quad y_{xxx}(L,t)=0, \tag{25}$$

where y_x, y_{xx}, and y_{xxx} are the first, second, and third partial derivatives of y with respect to x, respectively. The equation of motion is nondimensionalized with the following change of variables

$$Y=\frac{y}{L},\quad X=\frac{x}{L},\quad T=t\Omega.$$

By introducing the nondimensional velocity, mass fraction and frequency as follows:

$$u=\left(\frac{M}{EI}\right)^{1/2}\overline{U}L,\quad \beta=\frac{M}{m+M},\quad \omega=\left(\frac{M+m}{EI}\right)^{1/2}\Omega L^2,$$

and assuming a separable form for $Y(X,T)$ such that

$$Y(X,T)=\phi(X)e^{-i\omega T}, \tag{26}$$

it is possible to get the nondimensional equation of motion and boundary conditions

$$\frac{d^4\phi}{dX^4}+\mu u^2\frac{d^2\phi}{dX^2}+2\beta^{1/2}ui\omega\frac{d\phi}{dX}-\omega^2\phi=0, \tag{27}$$

$$\phi(0)=0,\quad \phi_X(0)=0,\quad \phi_{XX}(1)=0,\quad \phi_{XXX}(1)=0, \tag{28}$$

where ϕ_X, ϕ_{XX}, and ϕ_{XXX} are the first, second, and third derivatives of ϕ, respectively. The solution of ϕ is assumed to be of the form $\phi(X)=Ae^{zX}$ and this yields the characteristic polynomial

$$z^4+\mu u^2z^2+2\beta^{1/2}ui\omega z-\omega^2=0. \tag{29}$$

For specific values of μ, u and β, Eq. (29) provides four roots, z_n, $n=1,2,3,4$, where $z_n=z_n(\omega)$. The complete solution of $\phi(X)$ has the form

$$\phi(X)=A_1e^{z_1X}+A_2e^{z_2X}+A_3e^{z_3X}+A_4e^{z_4X}. \tag{30}$$

The solution of Eq. (30) based on the boundary conditions in Eq. (28) results in the complete solution

$$Y(X,T)=\sum_{n=1}^{4}A_ne^{z_nX}e^{i\omega T}=\sum_{n=1}^{4}A_n\underbrace{e^{\mathrm{Re}[z_n]X}}_{\text{(i)}}\underbrace{e^{i(\mathrm{Im}[z_n]X+\mathrm{Re}[\omega]T)}}_{\text{(ii)}}\underbrace{e^{-\mathrm{Im}[\omega]T}}_{\text{(iii)}}. \tag{31}$$

An inspection of the above equation indicates that $Y(X,T)$ is a product of three exponential terms of which the first term is bounded since X is bounded and the second term is oscillatory since the exponent is imaginary. The third term can grow unbounded with time if $\mathrm{Im}[\omega]<0$ and this represents unstable dynamics of the pipe. The exact mode and velocity at which the fluid-conveying pipe becomes unstable depends on the fluid mass fraction β.

4.2. Determination of momentum correction factor

For laminar flow, the Poiseuille solution of Navier–Stokes equation holds (Potter and Foss, 1982) and the value of μ can be determined analytically to be equal to 4/3. For turbulent flow, the value of μ approaches unity as the value of Reynolds number approaches infinity. Numerical values of μ for turbulent flow were calculated based on Eq. (23) using velocity profiles generated by the commercial software STAR-CCM.[2] The literature (Benedict, 1980) commonly cites a single value of μ for turbulent flow; the values cited are derived using assumptions that are better suited to high-Reynolds number turbulence. Since the modeling presented in Section 3.1 relaxes the assumption of high-Reynolds number turbulence, it is necessary to use a flow model with improved resolution near turbulent transition. Even with this improved resolution, knowledge of μ is required for more values of the Reynolds number than are feasible to simulate. To predict the value of μ for laminar, transition, and turbulent flow regimes, we use the following curve-fit:

$$\mu(\mathrm{Re})=\begin{cases}4/3 & \mathrm{Re}\le 2200,\\ 3.647-0.001052\times\mathrm{Re} & 2200<\mathrm{Re}<2413,\\ 1.04+167.2/\mathrm{Re} & \mathrm{Re}\ge 2413.\end{cases} \tag{32}$$

It can be seen from Fig. 4 that the data points obtained from simulation matches well with the expression of μ in Eq. (32). The choice of $2200<\mathrm{Re}<2413$ to define the "transition region" is somewhat arbitrary, as might be the choice of using one single value for μ to represent a phenomenon as complex as turbulent transition. However, the authors note that for a given flow setup the range of velocities corresponding to transition flow is small, making the choice of the transition model relatively unimportant.[3]

From the expressions for the nondimensional velocity and the Reynolds number, we get for a circular pipe

$$u=\left(\frac{M}{EI}\right)^{1/2}\overline{U}L,\quad \mathrm{Re}=\frac{\overline{U}D}{\nu}\ \Rightarrow\ u=\nu L\,\mathrm{Re}\sqrt{\frac{\pi\rho_f}{4EI}}. \tag{33}$$

[2] A product of CD-Adapco.

[3] The laminar to turbulent transition region can be seen in the Argand diagram in Fig. 5.

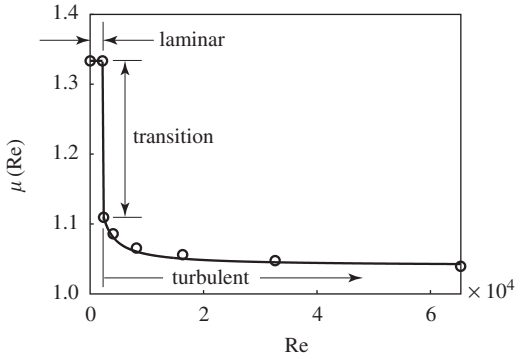

Fig. 4. Plot of the momentum correction factor μ as a function of the Reynolds number. The data points obtained through simulation are shown by circles.

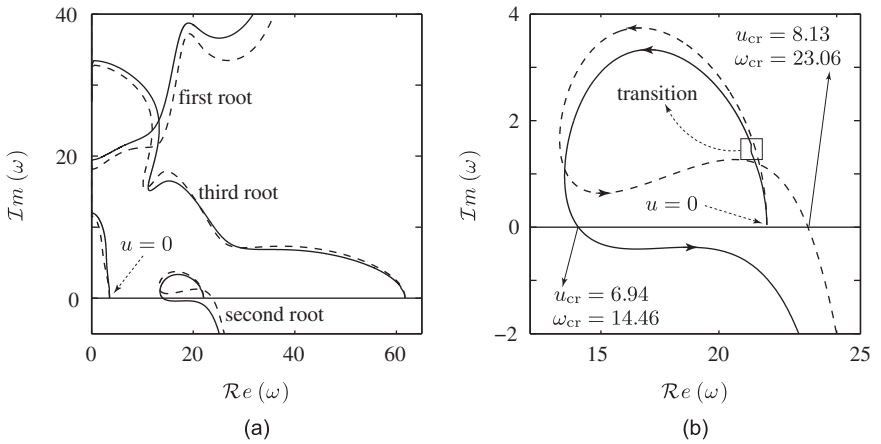

Fig. 5. (a) Locus of the first three roots of Det($\mathbf{Z}$) = 0 for uniform (dashed line) and non-uniform (solid line) flow models with $\beta = 0.3$. (b) A magnified image of the second root loci in (a).

Clearly, a value of u does not uniquely determine the Reynolds number. The geometric properties of the pipe (L, E, I) and density and kinematic viscosity of the working fluid (ρ_f, v) should be specified to determine the Reynolds number for a given u. Since the momentum correction factor μ is a function of the Reynolds number, it follows that the value of μ cannot be determined from the value of u alone.

5. Uniform and non-uniform flow model comparison

5.1. Turbulent flow

The locus of the first three roots of Det($\mathbf{Z}$) = 0 is shown in the Argand diagram in Fig. 5(a) for $\beta = 0.308$ for both uniform and non-uniform flow models. Since the fluid-conveying pipe undergoes flutter instability in the second mode, a separate Argand diagram of the loci of the second root is shown in Fig. 5(b). The root loci for the uniform flow model are a function of u alone (μ is implicitly assumed to be unity) but they are a function of both u and μ for the non-uniform flow model. As noted in Section 4.2, the value of μ is not uniquely defined in terms of u. Certain dimensional coefficients related to the working fluid and pipe geometry must be assumed to obtain this relationship. The non-uniform flow model assumes water to be the working fluid ($\rho_f = 1000\,\mathrm{kg/m^3}$, $v = 1.0 \times 10^{-6}\,\mathrm{m^2\,s}$) and the following parameters for the pipe:

$$E = 1.7\,\mathrm{MPa}, \quad I = 6.48 \times 10^{-10}\,\mathrm{m^4}, \quad L = 0.5\,\mathrm{m}. \tag{34}$$

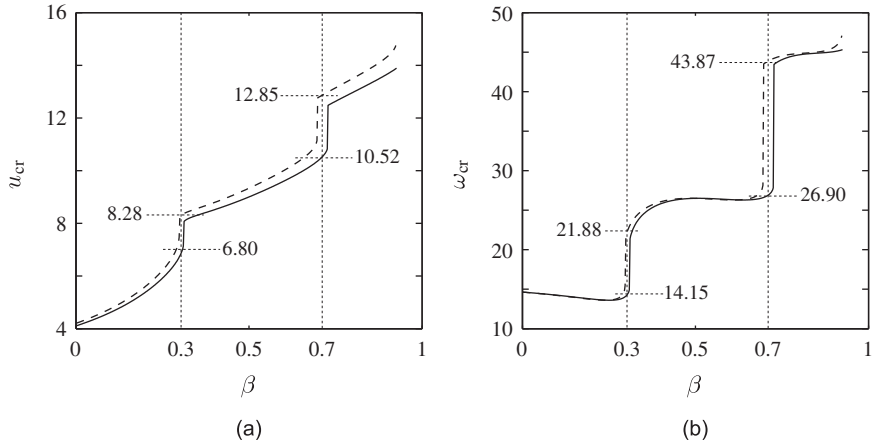

Fig. 6. Plot of (a) u_{cr} and (b) ω_{cr} for uniform (dashed line) and non-uniform (solid line) turbulent flow for different values of β.

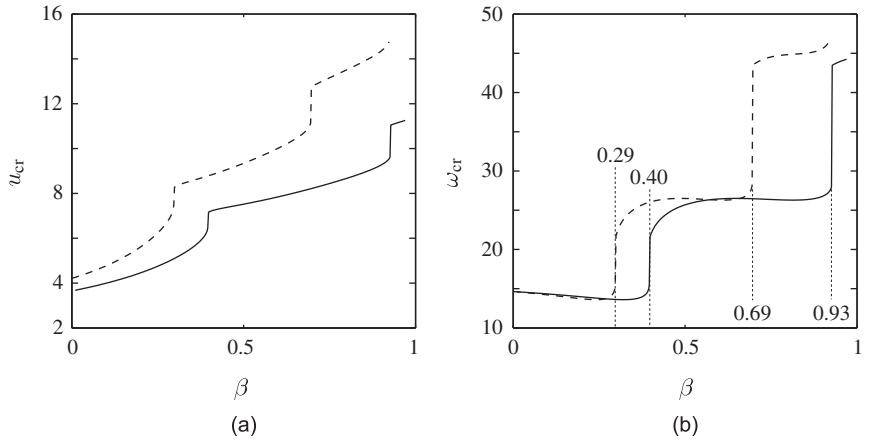

Fig. 7. Plot of (a) u_{cr} and (b) ω_{cr} for uniform (thin line) and laminar (thick line) flow for different values of β.

It is acknowledged that the need to specify dimensional parameters is a limitation but this limitation is not significant. An inspection of Fig. 4 reveals that μ is weakly related to the Reynolds number for turbulent flow and therefore dependence of μ on the dimensional parameters is not significant.

It can be seen from Fig. 5 that the root loci for the uniform and non-uniform flow models are quite different, though their μ values are quite similar.[4] A close look at the second-mode root loci indicates that the uniform flow model predicts flutter instability of the pipe to occur for a critical velocity of $u_{cr} = 8.13$ with $\omega_{cr} = 23.06$, whereas the non-uniform flow model predicts significantly lower values of $u_{cr} = 6.94$ (15% lower) and $\omega_{cr} = 14.46$ (37% lower). Clearly, the dynamics of the system are very sensitive to the value of μ in the neighborhood of $\beta = 0.3$. The values of u_{cr} and ω_{cr} are plotted in Fig. 6 for different values of β. This figure indicates that the non-uniform flow model predicts significantly lower values of u_{cr} and ω_{cr} for β in the neighborhood of 0.7 as well. There is good agreement between the uniform and non-uniform turbulent flow models for values of β that are not in the neighborhood of 0.3 or 0.7.

5.2. Laminar flow

In prior work, the plug flow model implicitly made the assumption that $\mu = 1$. It is clear from Fig. 4 that this assumption is reasonable only for high Reynolds number. The non-unique relationship between u and Re allows situations where this assumption is not reasonable. For example, inspection of Eq. (33) reveals that a sufficiently long

[4]The value of μ is implicitly assumed to be unity for the uniform flow model, whereas it has values in the neighborhood of 1.05 for the non-uniform flow model.

pipe could have a large value for u at low Reynolds number. A sufficiently long fluid-conveying pipe could therefore undergo flutter instability with laminar flow, in which case $\mu = 4/3$. In the case of turbulent flow, the near-unity value of μ yields values of u_{cr} and ω_{cr} which differ significantly from the uniform case only in certain thin regions of the β parameter space. Fig. 7 is analogous to Fig. 6, but assumes laminar flow and gives a very different result. The values of u_{cr} for laminar flow are quite different from that of uniform flow in all regions of the parameter space. The values of ω_{cr} for laminar flow are similar to that of uniform flow over much of the range of β but there are certain regions where the predicted values are significantly different. Unlike the thin regions near $\beta = 0.3$ and 0.7 for turbulent flow (see Fig. 6), the regions of large separation for laminar flow extend from approximately $\beta = 0.29$ to 0.40 and from $\beta = 0.69$ to 0.93.

6. Concluding remarks

The stability of cantilever pipes conveying fluid with a fully developed non-uniform velocity profile was assessed. The relevant equation of motion, derived herein, is tractable, requiring only the use of a single empirical parameter, μ, which accounts for the dependance of fluid momentum on the square of the fluid velocity. A sample method for the determination of μ is described. In previous analyses, which assumed a uniform velocity profile, this parameter was implicitly assumed to be unity. While this is a reasonable approximation at high Reynolds number, $\mu = 1$ is the minimum value possible, which is approached only in the limit of infinite Reynolds number. That is, the average momentum flux per unit mass for real fluid flows will always be greater than the uniform case, and the uniform profile assumption becomes monotonically less accurate as the Reynolds number decreases. This is particularly true in the case of laminar flow, where the value of μ reaches its maximum value. It was shown that the dependence of u, the nondimensional velocity relevant to the stability of the pipe, is not uniquely dependent on the Reynolds number. Thus, a large value of u may be attained at a relatively low Reynolds number.

The stability characteristics of a sample pipe were assessed with our updated model. In this pipe, the fluid became turbulent at relatively low u with the effect that $\mu \approx 1.05$ when u approached values necessary to achieve flutter instability. This proximity to the uniform model causes similarity between the predictions over much of the parameter space. However, there are significant differences in certain sensitive regions of the parameter space. A pipe with dimensions such that the conveyed fluid is laminar at the onset of flutter instability exhibited markedly different stability characteristics from the uniform case. Both the critical velocity and critical frequency were significantly different over large regions of the parameter space.

The authors believe that this updated model is a worthy addition to the body of literature on fluid-conveying pipes if for no reason other than its tractability. The equations of motion are no more difficult to solve than those of the uniform case for a known value of μ. While the accurate assessment of μ is nontrivial, it can be evaluated *a priori* for the entire range of flow velocities. Finally, the similarity of this model to the uniform flow model allows prior work to be updated easily. The predictions of instability of pinned–pinned and clamped–clamped pipes, and pipes with coaxially flowing external fluid may also be corrected with our model.

Acknowledgement

The support provided by the Office of Naval Research, ONR Grant no. N00014-08-1-0460, is gratefully acknowledged.

References

Ashley, H., Haviland, G., 1950. Bending vibrations of a pipeline containing fluid. Journal of Applied Mechanics 17, 229–232.

Bajaj, A.K., Sethna, P.R., Lundgren, T.S., 1980. Hopf bifurcation phenomena in tubes carrying fluid. SIAM Journal of Applied Mathematics 39, 213–230.

Benedict, R.P., 1980. Fundamentals of Pipe Flow. John Wiley and Sons, New York, NY.

Bourrières, F.-J., 1939. Sur en phenomene doscillation auto entrenue en mecanique des fluides reels. Publications Scientifiques et Techniques du Ministère de l'Air 147.

Feodoseev, V.P., 1951. Vibrations and stability of a pipe when liquid flows through it. Inzhenernyi Sbornik 10, 169–170.

Gregory, R.W., Païdoussis, M.P., 1966. Unstable oscillation of tubular cantilevers conveying fluid I. Theory. Proceedings of the Royal Society (London) 293, 512–527.

Hannoyer, M.J., Païdoussis, M.P., 1978. Instabilities of tubular beams simultaneously subjected to internal and external axial flows. ASME Journal of Mechanical Design 100, 328–336.
Holmes, P.J., 1978. Pipes supported at both ends cannot flutter. Journal of Applied Mechanics 45, 619–622.
Housner, G.W., 1952. Bending vibrations of a pipe line containing flowing fluid. Journal of Applied Mechanics 19, 205–208.
Lundgren, T.S., Sethna, P.R., Bajaj, A.K., 1979. Stability boundaries for flow induced motions of tubes with an inclined terminal nozzle. Journal of Sound and Vibration 64, 553–571.
Païdoussis, M.P., 1998. Fluid–Structure Interactions: Slender Structures and Axial Flow, vol. 1. Academic Press, London, UK.
Païdoussis, M.P., Issid, N.T., 1974. Dynamic stability of pipes conveying fluid. Journal of Sound and Vibration 33, 267–294.
Païdoussis, M.P., Laithier, B.E., 1976. Dynamics of Timoshenko beams conveying fluid. Journal of Mechanical Engineering Science 18, 210–220.
Païdoussis, M.P., Li, G.X., 1993. Pipes conveying fluid: a model dynamical problem. Journal of Fluids and Structures 7, 137–204.
Potter, M.C., Foss, J.F., 1982. Fluid Mechanics. Great Lakes Press, Okemos, MI.

Note from the Editor

It is remarkable that it took 48 years since Brooke Benjamin's seminal papers before the effect of a nonuniform velocity profile on the dynamics of pipes conveying fluid was tackled for the first time [the paper by Guo et al. (2010)[5] in this very issue of JFS]. Yet, hardly a month later, a second paper on the same subject was submitted, coincidently (and most appropriately) also to JFS: the present paper. These two papers use different approaches; hence there was no impediment to publication of both. However, this underlines how things are accelerating in research publications!

[5]C.Q. Guo, C.H. Zhang, M.P. Païdoussis, 2010. Modification of equation of motion of fluid-conveying pipe for laminar and turbulent flow profiles. Journal of Fluids and Structures 26(5), this issue.